Untwisting a Helically Coordinated Hexaazamacrocycle: Divalent Mg, Ca, Sr, Cd, Hg, and Pb Complexes of $(pyo)_2$[18]dieneN_6 and the X-ray Crystal Structure of the Cd Complex

L. Henry Bryant, Jr., Abdessadek Lachgar, and Susan C. Jackels*

Department of Chemistry, Wake Forest University, Winston-Salem, North Carolina 27109

Received November 22, 1994[⊗]

The synthesis and structural characterization of divalent Mg, Ca, Sr, Cd, Hg, and Pb complexes of $(pyo)_2$[18]-dieneN_6 (3,6,14,17,23,24-hexaazatricyclo[17.3.1.1^{8,12}]tetracosa-1(23),8,10,12(24),19,21- hexaene) are reported. The complexes were isolated as triflate salts and characterized by elemental analyses, IR and NMR spectral studies, and, in the case of the Cd complex, by an X-ray crystal structure. The proton NMR spectra of all the complexes are consistent with D_2 symmetry in which the ligand is hexacoordinated in a meridional wrap with the pyridine groups twisted relative to each other and the $-CH_2NHC_2H_4NHCH_2-$ groups forming helical linkages connecting the pyridine groups. A comparison of the crystal structures of the Cd and Zn complexes reveals that as the size of the metal ion increases, the pyridine groups untwist and the helicity of the coordinated ligand decreases. The NMR spectra of all the complexes are interpreted in light of this effect, and molecular modeling is used to predict the structures of the Hg and Pb complexes, giving results consistent with the NMR studies and the untwisting effect. The results of the X-ray crystal structure of $[Cd((pyo)_2[18]dieneN_6)](CF_3SO_3)_2$ are as follows: formula, $CdC_{20}N_6H_{26}S_2O_6F_6$; monoclinic; *I2/m* space group, with $a = 9.6945(6)$, $b = 15.6656$ (17), and $c = 18.5115(11)$ Å, β, 91.392(5)°, and $Z = 4$, resulting in $R = 0.0410$, $R_w = 0.052$, and GoF = 1.24.

Introduction

Molecules which form assemblies having helical topology are of fundamental importance in nature, for example, in DNA and proteins, but examples of helical assemblies involving metals and cyclic molecules are rare. Newkome *et al.*[1] first reported the structures of cobalt and copper complexes of Me_4-$(pyo)_2$[18]dieneN_6 that have helical structures, but low yields prevented complete characterization. Recently, Rothermel *et al.*[2] synthesized and studied the 18-membered hexaazamacrocycle containing two pyridine and four secondary amine groups, $(pyo)_2$[18]dieneN_6, shown below.

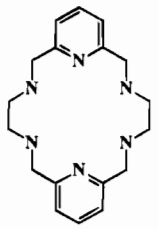

The crystal structure of $[Zn((pyo)_2[18]dieneN_6)](CF_3SO_3)_2$[3] revealed that $(pyo)_2$[18]dieneN_6 coordinates in a hexacoordinate pseudooctahedral meridional wrap, producing a helical complex with the two pyridine groups oriented at an angle of 104.5° relative to each other. The methylenic substituents on pyridine form the termini of two chains of atoms, including the ethylenediamine moieties, that form a double helix about zinc, connecting the 2- and 6-positions of the *trans* pyridine groups. The helical enantiomers thus produced have D_2 symmetry and stereochemistries at the amine nitrogen sites corresponding to *RRRR* or *SSSS* chirality. Since each enantiomer can twist helically in only one direction and is kinetically inert, this cyclic ligand yielded a single pair of optical isomers that was successfully resolved by fractional crystallization of diastereomeric salts with (+)-tartrate.[3] The two enantiomeric complexes correspond to twist and ethylenic conformations $\Lambda\delta\delta$ and $\Delta\lambda\lambda$.[4] Open-chain pentadentate complexes having a similar helical coordination geometry were found by Lindoy and Busch[5] from the 1:2 template condensation of 2,6-diacetylpyridine and 2-aminobenzenethiol on either Zn^{2+} or Cd^{2+}. Solution NMR studies confirmed that $[Zn((pyo)_2[18]dieneN_6)]^{2+}$ has a rigid helical structure identical to that observed in the solid state, giving detail in multiplet structure and coupling constants that could be accurately simulated using the crystallographic dihedral angles and the Karplus relationship.

In this paper we report the results of further synthetic and structural studies on the helical complexes of $(pyo)_2$[18]dieneN_6. In particular we are interested in how this remarkable ligand accommodates the large range of sizes of metal ions for which it forms very stable complexes.[2] Does the helix "untwist" to ultimately form approximately planar hexadentate coordinate geometry with large ions? Are the complexes highly symmetric, rigid, and kinetically inert on the NMR time scale? Can their structures be derived from the details of the NMR spectra, as was the case for $[Zn((pyo)_2[18]dieneN_6)]^{2+}$? To study these questions, we isolated the M^{2+} complexes of $(pyo)_2$[18]dieneN_6, where M is Mg, Ca, Sr, Cd, Hg, or Pb, as the triflate salt in each case. These metal complexes are diamagnetic with filled electronic shells and span the metal ionic radius sizes (six-coordinate) from 86 to 133 pm.[6] In this study the X-ray crystal structure of $[Cd((pyo)_2[18]dieneN_6)](CF_3SO_3)_2$ was determined. With this structure and the results of detailed NMR studies on the complexes, much can be learned about the structures, conformations, and properties of $(pyo)_2$[18]dieneN_6 complexes.

While this article was in preparation, Bligh *et al.* communicated their synthesis of the cyclohexanediamine analog of

[⊗] Abstract published in *Advance ACS Abstracts,* July 1, 1995.

(1) Newkome, G. R.; Majestic, V. K.; Fronczek, F. R. *Inorg. Chim. Acta* **1983**, *77*, L47−L49.
(2) Rothermel, G. L., Jr.; Miao, L.; Hill, A. L.; Jackels, S. C. *Inorg. Chem.* **1992**, *31*, 4854−4859.
(3) Bryant, L. H., Jr.; Lachgar, A.; Coates, K. S.; Jackels, S. C. *Inorg. Chem.* **1994**, *33*, 2219−2226.
(4) For nomenclature see: Leigh, G. J., Ed. *Nomenclature of Inorganic Chemistry*; Blackwell Scientific: Oxford, 1991; pp 182−185.
(5) Lindoy, L. F.; Busch, D. H. *Inorg. Chem.* **1974**, *13*, 2494−2498.
(6) Shannon, R. D. *Acta Crystallogr., Sect. A* **1976**, *A32*, 751−767.

0020-1669/95/1334-4230$09.00/0

$(pyo)_2$[18]dieneN_6 and the crystal structures of the zinc and cadmium complexes.[7] Thus, the generality of helical coordination in complexes related to $(pyo)_2$[18]dieneN_6 is demonstrated, as well as the untwisting effect of increasing metal ion size.

Experimental Section

Preparations. $(pyo)_2$[18]dieneN_6·$4CF_3SO_3H$ and $(pyo)_2$[18]dieneN_6·H_2O were prepared by the previously published methods.[2] All metal oxides and carbonates and other chemicals were reagent grade and were used as purchased.

Metal Triflate Salts. $[Cd(CF_3SO_3)_2 \cdot nH_2O]$,[8] $[Hg(CF_3SO_3)_2 \cdot nH_2O]$,[9] and $[Mg(CF_3SO_3)_2 \cdot nH_2O]$[10] were prepared on the basis of modifications of reported preparations in which an aqueous suspension of the appropriate metal oxide was reacted with trifluoromethanesulfonic acid. The resulting solutions were evaporated under reduced pressure, and the white solids obtained were recrystallized from acetonitrile. The products were confirmed by comparing the IR spectral data to the literature values. The hydration numbers were not determined. $[Ca(CF_3SO_3)_2 \cdot nH_2O]$,[11] $[Sr(CF_3SO_3)_2 \cdot nH_2O]$,[12] and $[Pb(CF_3SO_3)_2 \cdot nH_2O]$[13] were prepared from their carbonates by a similar procedure.

(3,6,14,17,23,24-Hexaazatricyclo[17.3.1.1^{8,12}]tetracosa-1(23),8,10,12(24),19,21-hexaene)magnesium(2+) Trifluoromethanesulfonate {[Mg((pyo)$_2$[18]dieneN$_6$)](CF$_3$SO$_3$)$_2$}. $[Mg(CF_3SO_3)_2 \cdot nH_2O]$ (0.99 g, 3.08 mmol; based on anhydrous formula weight) was added to an aqueous suspension of $(pyo)_2$[18]dieneN_6 (1.00 g, 3.08 mmol). The mixture was heated for 4 h. After the solution was cooled to room temperature, colorless crystals formed. The crystals were isolated and dried under vacuum. Yield: 0.92 g (46%). Mp = 308 °C dec. ^{1}H NMR (DMSO/TMS (ppm)): δ = 2.08 (m, 4H), 2.82 (m, 4H), 3.91 (d, J = 16.0 Hz, 4H), 4.32 (d, J = 5.2 Hz, 4H), 4.41 (br, 4H), 7.54 (d, J = 7.8 Hz, 4H), 8.10 (t, J = 7.8 Hz, 2H). ^{13}C{^{1}H} NMR (DMSO/TMS (ppm)): δ = 47.1, 50.7, 121.7, 141.1, 156.6. IR (KBr pellet (cm^{-1})): ν_{N-H} 3269 (s); ν_{C-H} 3092, 3024(w), 2924, 2884 (m); $\nu_{C=C,C=N}$ 1612, 1584, 1463, 1443 (m); $\nu_{S=O}$ 1296, 1244, 1222, 1024 (s); ν_{C-F} 1165 (s); $\delta_{S=O}$ 639 (s). Aqueous molar conductivity (10^{-3} M, 25 °C): 208 cm^2 ohm^{-1} mol^{-1}. Anal. Calcd for $MgC_{20}H_{26}N_6F_6O_6S_2$: Mg, 3.74; C, 37.02; H, 4.03; N, 12.95. Found: Mg, 3.67; C, 36.61; H, 3.97; N, 13.24.

(3,6,14,17,23,24-Hexaazatricyclo[17.3.1.1^{8,12}]tetracosa-1(23),8,10,12(24),19,21-hexaene)calcium(2+) Trifluoromethanesulfonate {[Ca((pyo)$_2$[18]dieneN$_6$)](CF$_3$SO$_3$)$_2$}. $[Ca(CF_3SO_3)_2 \cdot nH_2O]$ (1.01 g, 3.00 mmol; based on anhydrous formula weight) was added to an aqueous suspension of $(pyo)_2$[18]dieneN_6 (0.98 g, 3.00 mmol). The mixture was heated for 4 h. After the solution was cooled to room temperature, colorless crystals formed. The crystals were isolated and dried under vacuum. Yield: 1.4 g (70%). Mp = 308 °C dec. ^{1}H NMR (DMSO/TMS (ppm)): δ = 2.50 (br, 8H), 3.14 (br, 4H), 3.86 (br, 8H), 7.30 (d, J = 7.6 Hz, 4H), 7.83 (t, J = 7.6 Hz, 2H). ^{13}C{^{1}H} NMR (DMSO/TMS (ppm)): δ = 48.6, 54.0, 120.3, 138.6, 159.3. IR (KBr pellet (cm^{-1})): ν_{N-H} 3280 (s); ν_{C-H} 3069, 3011 (w), 2965, 2897, 2860 (m); $\nu_{C=C,C=N}$ 1600, 1578, 1458, 1445 (m); $\nu_{S=O}$ 1285, 1249, 1227, 1040 (s); ν_{C-F} 1196 (s); $\delta_{S=O}$ 635 (s). Anal. Calcd for $CaC_{20}H_{26}N_6F_6O_6S_2$: Ca, 6.03; C, 36.14; H, 3.94; N, 12.64. Found: Ca, 6.10; C, 36.36; H, 4.04; N, 12.56.

(3,6,14,17,23,24-Hexaazatricyclo[17.3.1.1^{8,12}]tetracosa-1(23),8,10,12(24),19,21-hexaene)strontium(2+) Trifluoromethanesulfonate {[Sr((pyo)$_2$[18]dieneN$_6$)](CF$_3$SO$_3$)$_2$}. $[Sr(CF_3SO_3)_2 \cdot nH_2O]$ (1.08 g, 2.80 mmol) was added to an aqueous suspension of $(pyo)_2$[18]dieneN_6 (0.92 g, 2.80 mmol). The mixture was heated for 4 h. After the solution was cooled to room temperature, colorless crystals formed. The crystals were collected and dried under vacuum. Yield: 1.3 g (65%). Mp = 285 °C dec. ^{1}H NMR (DMSO/TMS (ppm)): δ = 2.75 (s, 12H), 3.92 (d, J = 3.4 Hz, 8H), 7.29 (d, J = 7.6 Hz, 4H), 7.84 (t, J = 7.6 Hz, 2H). ^{13}C{^{1}H} NMR (DMSO/TMS (ppm)): δ = 48.4, 54.0, 120.7, 138.0, 158.9. IR (KBr pellet (cm^{-1})): ν_{N-H} 3311, 3276 (s); ν_{C-H} 3073, 2965, 2900, 2864 (m); $\nu_{C=C,C=N}$ 1599, 1578, 1463, 1458 (m); $\nu_{S=O}$ 1302, 1244, 1241, 1031 (s); ν_{C-F} 1158 (s); $\delta_{S=O}$ 637 (s). Anal. Calcd for $SrC_{20}H_{26}N_6F_6O_6S_2$: Sr, 12.30; C, 33.72; H, 3.67; N, 11.79. Found: Sr, 12.70; C, 33.71; H, 3.68; N, 11.82.

(3,6,14,17,23,24-Hexaazatricyclo[17.3.1.1^{8,12}]tetracosa-1(23),8,10,12(24),19,21-hexaene)cadmium(2+) Trifluoromethanesulfonate {[Cd((pyo)$_2$[18]dieneN$_6$)](CF$_3$SO$_3$)$_2$}. $[Cd(CF_3SO_3)_2 \cdot nH_2O]$ (0.61 g, 1.5 mmol; based on anhydrous formula weight) was added to a methanolic solution of $(pyo)_2$[18]dieneN_6·$4CF_3SO_3H$ (1.4 g, 1.5 mmol). The pH of the solution was adjusted to neutrality (determined by pH paper) with triethylamine. After the addition, a white solid precipitated. The crude product was dissolved in 20 mL of boiling methanol. After the solution was filtered and cooled to room temperature, colorless crystals formed. The crystals were isolated and dried under vacuum. Yield: 0.52 g (47%). Mp = 230 °C dec. ^{1}H NMR (DMSO/TMS (ppm)): δ = 2.11 (m, 4H), 2.97 (m, 4H), 3.95 (d, J = 16.4 Hz, 4H), 4.18 (d of d, J = 5.2 Hz, 4H), 4.33 (br, 4H), 7.51 (d, J = 7.8 Hz, 4H), 8.08 (t, J = 7.8 Hz, 2H). ^{13}C{^{1}H} NMR (DMSO/TMS (ppm)): δ = 47.9, 49.2, 123.1, 140.6, 154.6. IR (KBr pellet (cm^{-1})): ν_{N-H} 3269 (s); ν_{C-H} 3084 (w), 2930, 2912, 2881 (m); $\nu_{C=C,C=N}$ 1606, 1587, 1465, 1437 (m); $\nu_{S=O}$ 1294, 1244, 1221, 1026 (s); ν_{C-F} 1161 (s); $\delta_{S=O}$ 636 (s). Aqueous molar conductivity (10^{-3} M, 25 °C): 232 cm^2 ohm^{-1} mol^{-1}. Anal. Calcd for $CdC_{20}H_{26}N_6F_6O_6S_2$: Cd, 15.25; C, 32.60; H, 3.56; N, 11.40. Found: Cd, 15.15; C, 32.36; H, 3.56; N, 11.27.

(3,6,14,17,23,24-Hexaazatricyclo[17.3.1.1^{8,12}]tetracosa-1(23),8,10,12(24),19,21-hexaene)mercury(2+) Trifluoromethanesulfonate {[Hg((pyo)$_2$[18]dieneN$_6$)](CF$_3$SO$_3$)$_2$}. $[Hg(CF_3SO_3)_2 \cdot nH_2O]$ (1.20 g, 2.4 mmol; based on anhydrous formula weight) was added to an aqueous suspension of $(pyo)_2$[18]dieneN_6 (0.79 g, 2.4 mmol). The mixture was heated for 1 h. After the solution was filtered and cooled to room temperature, colorless crystals formed. The crystals were isolated and dried under vacuum. Yield: 1.4 g (70%). Mp = 188 °C dec. ^{1}H NMR (DMSO/TMS (ppm)): δ = 2.15 (m, 4H), 3.07 (m, 4H), 4.09 (s, 8H), 4.46 (br, 4H), 7.53 (d, J = 7.6 Hz, 4H), 8.09 (t, J = 7.6 Hz, 2H). ^{13}C{^{1}H} NMR (DMSO/TMS (ppm)): δ = 47.7, 123.6, 140.0, 152.9. IR (KBr pellet (cm^{-1})): ν_{N-H} 3271 (s); ν_{C-H} 3083 (w), 2956, 2928, 2878, 2851 (m); $\nu_{C=C,C=N}$ 1604, 1589, 1464, 1433 (m); $\nu_{S=O}$ 1294, 1244, 1220, 1027 (s); ν_{C-F} 1160 (s); $\delta_{S=O}$ 638 (s). Anal. Calcd for $HgC_{20}H_{26}N_6F_6O_6S_2$: C, 29.11; H, 3.17; N, 10.18. Found: C, 29.17; H, 3.17; N, 10.12.

(3,6,14,17,23,24-Hexaazatricyclo[17.3.1.1^{8,12}]tetracosa-1(23),8,10,12(24),19,21-hexaene)lead(2+) Trifluoromethanesulfonate {[Pb((pyo)$_2$[18]dieneN$_6$)](CF$_3$SO$_3$)$_2$}. $[Pb(CF_3SO_3)_2 \cdot nH_2O]$ (1.21 g, 2.40 mmol; based on anhydrous formula weight) was added to an aqueous suspension of $(pyo)_2$[18]dieneN_6 (0.78 g, 2.40 mmol). The mixture was heated for 4 h. After the solution was cooled to room temperature, colorless crystals formed. The crystals were collected and dried under vacuum. Yield: 1.2 g (60%). Mp = 273 °C dec. ^{1}H NMR (DMSO/TMS (ppm)): δ = 2.84 (s, 8H), 3.85 (s, 4H), 4.23 (d, J = 5.4 Hz, 8H), 7.47 (t, J = 7.6 Hz, 4H), 7.97 (t, J = 7.6 Hz, 2H). ^{13}C{^{1}H} NMR (DMSO/TMS (ppm)): δ = 48.6, 53.0, 121.3, 139.2, 159.6. IR (KBr pellet (cm^{-1})): ν_{N-H} 3374, 3338, 3283, 3245 (m); ν_{C-H} 3060 (w), 2895 (br); $\nu_{C=C,C=N}$ 1597, 1579, 1457, 1444 (m); $\nu_{S=O}$ 1280, 1265, 1251, 1225, 1030 (s); ν_{C-F} 1155 (s); $\delta_{S=O}$ 638 (s). Anal. Calcd for $PbC_{20}H_{26}N_6F_6O_6S_2$: C, 28.88; H, 3.15; N, 10.10. Found: C, 28.98; H, 3.28; N, 10.12.

Characterization Methods. Elemental analyses were carried out by Galbraith Laboratories, Inc., Knoxville, TN. IR spectra were obtained on a Mattson 4020 FT-IR spectrophotometer using KBr pellets. Molar conductance measurements were obtained with a YSI Model 35 conductance meter and an immersion-type electrode. ^{1}H and ^{13}C NMR spectra were obtained on a Varian VXR-200 spectrometer.

[Cd((pyo)$_2$[18]dieneN$_6$)](CF$_3$SO$_3$)$_2$ Crystal Structure. A colorless 0.25 × 0.30 × 0.35 mm^3 crystal suitable for single-crystal X-ray diffraction was selected and mounted in a glass capillary. Three-

(7) Bligh, S. W. A.; Choi, N.; Evagorou, E. G.; Li, W.-S.; McPartlin, M. *J. Chem. Soc., Chem. Commun.* **1994**, 2399–2400.
(8) Boumizane, K.; Herzog-Cance, M. H.; Jones, D. J.; Pascal, J. L.; Potier, J.; Roziere, J. *Polyhedron* **1991**, *10*, 2757–2769.
(9) Persson, I.; Dash, K. C.; Kinjo, Y. *Acta Chem. Scand.* **1990**, *44*, 433–442.
(10) Corey, E. J.; Katsuichi, S. *Tetrahedron Lett.* **1983**, *24*, 169–172.
(11) Sugita, K.; Ohta, A.; Onaka, M.; Yusuke, I. *Bull. Chem. Soc. Jpn.* **1991**, *64*, 1792–1799.
(12) Bell, T. W.; Guzzo, F.; Drew, M. G. B. *J. Am. Chem. Soc.* **1991**, *113*, 3115–3122.
(13) Wendsjö, A.; Lindgren, J.; Paluszkiewicz, C. *Electrochim. Acta* **1992**, *37*, 1689–1693.

Table 1. ^{1}H NMR Spectral Data for $(pyo)_2$[18]dieneN$_6$ Complexes in DMSO-d_6 (δ, ppm)[a,b]

Zn	Cd	Mg	Ca	Sr	Pb	Hg	assignment
8.11, t J = 7.8	8.08, t J = 7.8	8.10, t J = 7.8	7.83, t J = 7.6	7.84, t J = 7.6	7.97, t J = 7.6	8.09, t J = 7.6	H_A
7.54, d J = 7.8	7.51, d J = 7.8	7.54, d J = 7.8	7.30, d J = 7.6	7.29, d J = 7.6	7.47, d J = 7.6	7.53, d J = 7.6	H_B
4.55, s	4.33, s	4.41, s	3.14, s	2.75, s	3.85, s	4.46, s	H_E
4.33, dd J = 16.8, J = 5.8	4.18, dd J = 16.4, J = 5.2	4.32, d J = 5.2	3.86, br	3.92, s	4.23, d J = 5.4	4.09, s	H_C
3.91, d J = 16.8	3.95, d J = 16.4	3.91, d J = 16.0	3.86, br	3.92, s	4.23, d J = 5.4	4.09, s	H_D
2.75, m	2.97, m	2.82, m	2.50, br	2.75, s	2.84, s	3.07, m	H_F
2.10, m	2.11, m	2.08, m	2.50, br	2.75, s	2.84, s	2.15, m	H_G

[a] Chemical shifts referenced to TMS at 0.00 ppm. [b] J values in hertz.

Table 2. ^{1}H NMR Spectral Data for Zn^{2+}, Cd^{2+}, Mg^{2+}, and Hg^{2+} $(pyo)_2$[18]dieneN$_6$ Complexes in D_2O (δ, ppm)[a,b]

Zn	Cd	Mg[c]	Hg	assignment
8.01, t J = 7.8	8.00, t J = 7.8	8.03, t J = 7.8	8.01, t J = 7.6	H_A
7.45, d J = 7.8	7.45, d J = 7.8	7.47, d J = 7.8	7.45, d J = 7.6	H_B
4.32, d J = 6.2	4.27, d J = 17.0	4.39, d J = 17.0	4.24, d J = 16.8	H_C
3.96, d J = 17.0	4.03, d J = 17.0	4.00, d J = 17.0	4.11, d J = 16.8	H_D
3.96, s				H_E
2.85, m	3.11, d J = 10.6	2.97, d J = 10.4	3.21, d J = 10.6	H_F
2.26, m	2.29, d J = 10.6	2.29, d J = 10.4	2.30, d J = 10.6	H_G

[a] Chemical shifts referenced to DSS at 0.00 ppm. [b] J values in hertz. [c] Chemical shifts for the free macrocycle resonances are not included.

Table 3. Chemical Shift Difference for Geminal Protons of $(pyo)_2$[18]dieneN$_6$ Complexes in D_2O (Hz)

Zn	Mg	Cd	Hg	difference
76	78	48	23	$\nu(H_C) - \nu(H_D)$
118	136	164	182	$\nu(H_F) - \nu(H_G)$

Table 4. Summary of Crystallographic Data for $[Cd((pyo)_2[18]dieneN_6)](CF_3SO_3)_2$

formula	$CdC_{20}N_6H_{26}S_2O_6F_6$
formula weight (g/mol)	736.97
crystal system	monoclinic
space group	*I*2/*m*
Z	4
a (Å)	9.6945(6)
b (Å)	15.6676(17)
c (Å)	18.5115(11)
β (deg)	91.392(5)
V (Å^3)	2810.9(4)
D_{calc} (g cm^{-3})	1.741
cryst dim (mm^3)	0.25 × 0.30 × 0.35
temp (°C)	25
radiation	Mo Kα
scan type	$2\theta-\omega$
octants collected	$\pm h,+k,+l$
reflns collected	5058
unique reflns with $I \geq 2.5\sigma(I)$	3082
absorption coeff (mm^{-1})	1.77
refined parameters	198
R	0.041
R_w	0.052
GoF	1.24

dimensional intensity data were collected at 25 °C on a Rigaku AFC6S diffractometer using Mo Kα radiation, λ = 0.70930 Å, and a graphite monochromator. Accurate unit cell parameters were obtained by least-squares refinement of the setting angle of 65 reflections in the range $40 < 2\theta < 45°$. Intensity data were collected using the $2\theta-\omega$ scan method up to 2θ = 59.9°. Three intensity control reflections were monitored every 200 reflections, resulting in no evidence of crystal deterioration or loss of alignment throughout data collection. A total of 5058 reflections were collected (h −13/13, k 0/22, l 0/26). A total of 3082 of the 4230 unique reflections had $I \geq 2.5\sigma(I)$ and were included in the refinement. No absorption correction was applied, due to the small magnitude of the linear absorption coefficient (μ = 1.77 mm^{-1}). Table 4 summarizes the most important crystallographic data. The structure was solved using the direct method program SOLVER of the NRCVAX package.[14] Subsequent least-squares refinement and difference Fourier maps yielded the positions of all the non-hydrogen atoms in the asymmetric unit. The hydrogen atoms attached to the amine nitrogen atoms of the macrocycle were located on a difference electron density map. The atomic positions of the remaining hydrogen atoms were calculated. Final least-squares refinement with hydrogen atoms contributing to the structure factor, anisotropic thermal parameters for all non-hydrogen atoms, and a statistical weighting scheme converged in three cycles to R = 0.041, R_w = 0.052, and GoF = 1.24. The maximum shift/σ ratio for all the 198 refined parameters was less than 0.001. A final difference Fourier map was featureless, with the deepest hole having a value of −1.2 e/Å^3 at 0.4 Å from S_2 and the highest residual of 1.1 e/Å^3 at 0.9 Å from Cd. Final atomic coordinates and their calculated standard deviations and the calculated positions for the hydrogen atoms are given in Table 5. Tables 6 and 7 also give selected bond distances, bond angles, and torsion angles. Complete tables and F_o/F_c tables are included in the supporting information.

Table 5. Atomic Parameters x, y, z in Fractions of the Unit Cell Dimensions and Isotropic Thermal Parameters for $[Cd((pyo)_2[18]dieneN_6](CF_3SO_3)_2$

atom	x	y	z	B_{iso}[a]
Cd	1/2	0.24738(5)	0	3.25(3)
N1	0.6945(5)	0.1627(3)	0.03527(25)	3.81(24)
N2	0.5108(5)	0.2421(3)	0.12472(21)	3.33(21)
N3	0.3138(5)	0.3281(3)	0.04556(24)	3.63(22)
C1	0.8095(6)	0.2248(4)	0.0307(3)	4.2(3)
C2	0.6767(7)	0.1279(4)	0.1099(4)	4.8(3)
C3	0.5985(6)	0.1877(4)	0.1575(3)	3.8(3)
C4	0.6087(7)	0.1839(5)	0.2330(3)	5.2(4)
C5	0.5239(8)	0.2359(6)	0.2717(3)	6.1(4)
C6	0.4366(7)	0.2908(4)	0.2378(3)	5.1(3)
C7	0.4319(6)	0.2934(4)	0.1624(3)	3.7(3)
C8	0.3435(7)	0.3576(4)	0.1196(3)	4.3(3)
C9	0.1956(6)	0.2696(4)	0.0407(3)	4.0(3)
S1	0.7370(3)	1/2	0.10144(16)	5.56(15)
O11	0.6944(6)	0.4222(3)	0.1338(3)	9.9(4)
O12	0.7230(9)	1/2	0.0248(4)	8.6(5)
C11	0.9157(14)	1/2	0.1110(7)	6.4(7)
F11	0.9555(8)	1/2	0.1838(4)	11.0(5)
F12	0.9746(5)	0.4326(3)	0.0872(3)	11.6(4)
S2	0.1474(5)	0	0.09918(18)	8.30(23)
O21	0.0631(6)	0.0768(3)	0.1026(3)	9.0(3)
O22	0.2666(11)	0	0.0412(4)	10.4(6)
C12	0.2712(10)	0	0.1425(8)	6.8(7)
F21	0.3289(6)	0.0695(3)	0.1765(3)	12.4(4)
F22	0.1912(12)	0	0.2298(5)	16.4(8)
H(N1)	0.698	0.113	−0.005	4.6
H(N3)	0.305	0.381	0.008	4.4

[a] B_{iso} is the mean of the principal axes of the thermal ellipsoid.

(14) Gabe, E. J.; LePage, Y.; Eharland, J.-P.; Lee, F. L.; White, P. S. *J. Appl. Crystallogr.* **1989**, *22*, 384−387.

Table 6. Selected Bond Distances (Å) and Angles (deg) in $[Cd((pyo)_2[18]dieneN_6)](CF_3SO_3)_2$[a]

	(a) Cadmium Environment		
Cd−N2	2.306(4)	Cd−N3	2.372(4)
Cd−N1	2.382(5)		
N2−Cd−N2a	176.02(17)	N1−Cd−N3a	78.16(16)
N2−Cd−N1	71.45(16)	Cd−N2−C3	119.4(3)
N2−Cd−N1a	106.23(16)	Cd−N1−C2	112.7(5)
N2−Cd−N3	71.48(14)	Cd−N1−C1	102.5(3)
N2−Cd−N3a	110.78(15)	Cd−N3−C9	103.9(3)
N1−Cd−N1a	112.62(17)	Cd−N3−C8	111.4(3)
N1−Cd−N3	142.93(16)		
	(b)Ligand($C_{18}H_{22}N_6$)		
N2−C3	1.340(7)	C5−C6	1.362(11)
N2−C7	1.328(7)	C4−C3	1.393(8)
N1−C2	1.483(8)	C3−C2	1.492(9)
N1−C1	1.476(8)	C1−C9a	1.505(8)
N3−C9	1.477(7)	C8−C7	1.516(8)
N3−C8	1.469(7)	C7−C6	1.391(8)
C5−C4	1.370(12)		
C3−N2−C7	121.2(4)	N2−C7−C6	120.4(6)
C2−N1−C1	112.7(5)	N2−C3−C2	117.0(5)
C9−N3−C8	112.9(4)	C4−C3−C2	122.5(6)
C4−C5−C6	120.8(5)	C8−C7−C6	122.7(5)
C5−C4−C3	118.2(6)	N1−C2−C3	112.9(5)
C5−C6−C7	118.9(6)	N1−C1−C9a	110.4(4)
N2−C3−C4	120.5(6)	N3−C9−C1a	111.0(4)
N2−C7−C8	116.8(4)		

[a] Atoms X and Xa are symmetry related by the 2-fold axis in Figure 3 that includes Cd and is perpendicular to the plane of the page.

Table 7. Selected Torsion Angles (deg) for $[Cd((pyo)_2[18]dieneN_6)](CF_3SO_3)_2$[a]

Cd−N1−C2−C3	−33.0(3)	N1−C1−C9a−N3a	69.8(3)
Cd−N3−C8−C7	−33.3(3)	H(N1)−N1−C2−H2b	89.1(5)
Cd−N1−C1−C9a	−50.0(3)	H(N1)−N1−C2−H2a	−287.7(2)
Cd−N3−C9−C1a	−44.8(3)	H(N1)−N1−C1−H1b	−60.6(4)
N2−C3−C2−N1	26.2(3)	H(N1)−N1−C1−H1a	−177.6(8)
N2−C7−C8−N3	25.3(3)		

[a] Atom numbers refer to Table 5.

Molecular Mechanics Calculations. The molecular mechanics force field used was MM2 (QCPE-395, 1977)[15,16] in its extended form and with the graphical interface and parameters of PCMODEL (hereafter referred to as MMX, obtained as version 4.0 of PCMODEL from Serena Software, Bloomington, IN). Except where noted, the parameters for the organic ligands were set to the PCMODEL default values. The force field about the metal ion was designed so that the metal−ligand distances and the ligating atom−ligating atom interactions determined the shape of the coordination sphere. This was accomplished by setting to zero the X−metal−X angle parameters, the torsional parameters involving the X−M−Y−Z and M−X−Y−Z bonds, and the van der Waals parameters of the metal atom. This method is very similar to the points-on-a-sphere model that has been used successfully for complexes of filled-shell alkali and alkaline-earth ions.[17]

In the MMX force field of PCMODEL, all M−X distances are scaled on the basis of the covalent radius of the metal ion.[18] For a given metal, this radius depends on its oxidation state, coordination number, and electronic spin state. PCMODEL M−X distance parameters are calibrated relative to Fe(III), tetrahedral and high spin, with $R = 1.26$ Å. The R values used for divalent Zn, Cd, Hg, and Pb were 1.51, 1.72, 1.91, and 2.06 Å, respectively, determined from a comparison of the Shannon and Prewitt[19] crystal radii for these ions with that for high-spin tetracoordinate Fe(III). The calculations were carried out on a Silicon Graphics Iris Indigo R4000 workstation using the coordinates of the Zn^{2+} $(pyo)_2[18]dieneN_4$ complex as the initial ones. The resulting structures, shown in Figure 5, gave results in the cases of Zn and Cd very close to the crystal structures (calculated pyridine twist angles were 105 and 91° versus 104.5 and 91.5° observed).

Results and Discussion

Syntheses. The Cd^{2+} complex of $(pyo)_2[18]dieneN_6$ was prepared by reaction of $(pyo)_2[18]dieneN_6{\cdot}4CF_3SO_3H$ with $Cd(CF_3SO_3)_2$ in methanol followed by neutralization with triethylamine. The Mg^{2+}, Ca^{2+}, Sr^{2+}, Hg^{2+}, and Pb^{2+} complexes were prepared by reaction of the neutral macrocyclic ligand with aqueous metal triflate salt. Recrystallization from methanol gave crystalline samples of analytical purity that contained no additional solvent. The compounds were characterized by elemental analyses, conductivity, IR spectroscopy, and NMR spectroscopy, and, for the Cd^{2+} compound, the X-ray crystal structure was determined. In aqueous solution, the Cd^{2+} and Mg^{2+} complexes behave as 2:1 electrolytes,[20] giving conductivities slightly below the range of 225−270 cm^2 ohm^{-1} $mole^{-1}$. This behavior is similar to that reported previously for the Zn^{2+} complex.[3]

Infrared Spectra. The IR spectral data obtained from KBr pellets and band assignments for $[M((pyo)_2[18]dieneN_6)](CF_3SO_3)_2$, where M is Mg, Cd, Ca, Sr, Hg, or Pb, are listed in the Experimental Section. Compared to the weak N−H stretching frequency of 3269 cm^{-1} for $(pyo)_2[18]dieneN_6$, the increase in the intensity of this band for each of the complexes indicates metal coordination to the secondary amines. $[Hg((pyo)_2[18]dieneN_6)](CF_3SO_3)_2$ and $[Ca((pyo)_2[18]dieneN_6)](CF_3SO_3)_2$ each exhibit a single N−H stretching frequency at 3271 and 3280 cm^{-1}, respectively, but $[Sr((pyo)_2[18]dieneN_6)](CF_3SO_3)_2$ and $[Pb((pyo)_2[18]dieneN_6)](CF_3SO_3)_2$ exhibit splitting of the N−H stretching band into two bands at 3311 and 3276 cm^{-1} for the Sr^{2+} complex and into several bands for the Pb^{2+} complex. For tetraamine macrocyclic complexes, interaction of additional anions in positions *cis* to the macrocyclic donors gives splittings of the N−H stretching bands.[21] Coordination of pyridine nitrogen to each metal ion is indicated by the shift of the high-energy pyridine band[22] from 1575 cm^{-1} in the spectrum of $(pyo)_2[18]dieneN_6$ to 1589, 1587, and 1584 cm^{-1} in the Zn, Cd, and Mg complexes, respectively. For the Hg^{2+}, Ca^{2+}, Sr^{2+}, and Pb^{2+} complexes, the high-energy pyridine band around 1600 cm^{-1} indicates coordination of the pyridine to the metal ions.[23] There are no bands at 1380 cm^{-1}, indicative of coordinated triflate,[24] for any of the complexes. Ionic triflate in the compounds is confirmed by two bands[25] at 1296 and 1244 cm^{-1} for each complex. The S=O and C−F bands are nearly invariant for the complexes. Also, the lack of bands attributable to solvent is consistent with the formulation of the compounds as anhydrous.

^{13}C NMR Spectra. The proton-decoupled spectrum of $[M((pyo)_2[18]dieneN_6)](CF_3SO_3)_2$, where M is Mg, Cd, Ca, Sr, Hg, or Pb, in either D_2O or DMSO-d_6 (see Experimental Section) exhibits only five ^{13}C resonances. This fact indicates

(15) Burkert, U.; Allinger, N. L. *Molecular Mechanics*, ACS Monograph 177; American Chemical Society; Washington, DC, 1982.
(16) Allinger, N. L. *J. Am. Chem. Soc.* **1977**, *99*, 8127.
(17) Hay, B. P.; Rustad, J. R. *J. Am. Chem. Soc.* **1994**, *116*, 6316.
(18) Kreek, T. Ph.D. Dissertation, Indiana University, Bloomington, IN, 1992.
(19) Shannon, R. D.; Prewitt, C. T. *Acta Crystallogr.* **1969**, *B25*, 925. Shannon, R. D. *Ibid.* **1976**, *A32*, 751.
(20) Geary, W. J. *Coord. Chem. Rev.* **1971**, *7*, 81−122.
(21) Poon, C.; Tang, T.; Che, C. *J. Chem. Soc., Dalton Trans.* **1983**, 1647−1651.
(22) Gill, N. S.; Nuttall, R. H.; Scaife, D. E.; Sharp, D. W. A. *J. Inorg. Nucl. Chem.* **1961**, *18*, 79−87.
(23) Dixon, N. E.; Jackson, W. G.; Lay, P. A.; Sargeson, A. M. *Inorg. Chem.* **1984**, *23*, 2940−2947.
(24) Dixon, N. E.; Jackson, W. G.; Lancaster, M. J.; Lawrance, G. A.; Sargeson, A. M. *Inorg. Chem.* **1981**, *20*, 470−476.
(25) Dixon, N. E.; Jackson, W. G.; Lay, P. A.; Sargeson, A. M. *Inorg. Chem.* **1984**, *23*, 2940−2947.

that the four quadrants of the macrocycle are chemically and magnetically equivalent in the complex. In order to achieve this, the macrocycle must be twisted symmetrically in a meridional mode about M^{2+}, yielding a complex with D_2 symmetry. Only one of the five possible NH isomers for $(pyo)_2$-[18]dieneN_6, the one with stereochemistry at the amine nitrogen sites corresponding to *RRRR* or *SSSS* chirality[26] when coordinated, has three C_2 rotational axes and is capable of twisting to make a meridional pseudooctahedral complex having D_2 symmetry. Addition of excess free ligand to a D_2O solution of each complex produced a spectrum showing superposition of free and complexed ligand, indicating that ligand exchange is slow on the time scale of the NMR experiment. Additionally, there were no changes in the chemical shifts of the carbon resonances even after several months in solution, consistent with the known thermodynamic stability of the complexes.[2] Relative to the protonated free ligand, the α, γ, and β carbons of the pyridine ring are slightly shifted alternating in sign, positive for α and γ and negative for β. Similar shift patterns have been reported for N-protonated pyridine.[27] The largest observed shifts relative to free ligand are for the carbon atoms of the ethylenic linkage, which are shifted upfield by about 5 ppm. In contrast, the methylenic carbon adjacent to pyridine is shifted downfield by about 0.5 ppm.

^{1}H NMR Spectra in DMSO-d_6. ^{1}H NMR spectral data for the Zn^{2+}, Cd^{2+}, Mg^{2+}, Ca^{2+}, Sr^{2+}, Pb^{2+}, and Hg^{2+} $(pyo)_2$[18]-dieneN_6 complexes in DMSO-d_6 are listed in Table 1, and representative spectra are shown in Figure 1. Addition of $(pyo)_2$-[18]dieneN_6·4CF_3SO_3H to each solution produced a spectrum showing superposition of free and complexed macrocyclic ligand, indicating that both metal ion and N−H exchange are slow on the NMR time scale. The assignments for the spectra correspond to the labeling shown in Figure 1. The spectra of these three complexes are similar in many regards, so the spectra will at first be discussed collectively and then the individual differences will be addressed.

In all cases, the fact that only one pattern is observed for each of H_A through H_G indicates that the four quadrants of the macrocyclic ligand are chemically equivalent. In order to achieve this, the macrocycle must be twisted symmetrically, albeit possibly to a different degree in each complex, in a meridional mode, as was observed for the Zn^{2+} complex. The resolution of geminal protons into separate multiplets shows that the $\Delta\lambda\lambda$ ($\Lambda\delta\delta$) enantiomeric forms are not rapidly interconverting in solution on the time scale of the NMR experiment.

The pyridine hydrogens H_A and H_B exhibit the expected triplet and doublet splitting patterns and chemical shifts. The amine hydrogens H_E appear as a broad resonance due to the proximity of the nitrogen quadrupolar nucleus, the shape of which is indicative of a large ratio of ^{14}N relaxation rate to N−H coupling.[28] Hydrogens H_C and H_D are chemically and magnetically nonequivalent, and with H_E, they form an ABX spin system,[29] where X is H_E. The hydrogen H_D appears as a doublet, whereas H_C appears as a doublet of doublets (partly overlapping H_E). A homonuclear correlation spectroscopy (COSY) spectrum showed that H_D is coupled to H_C, whereas H_C is coupled to H_D and H_E. In addition, a homonuclear decoupling experiment in which H_E is irradiated resulted in the collapse of the doublet of doublets for H_C into a single doublet ($J_{CD} = J_{DC}$) with no concomitant effect on H_D. This observation can be understood by examining the stereochemistry about the nitrogen and the methylenic carbon atoms. The Karplus equation[30]

$$^3J_{H-H} = 8.5 \cos^2 \Phi - 0.28$$

is used to predict the dihedral angle (Φ) from the known vicinal coupling constants. The Newman projection for the complexes, viewed down the nitrogen−carbon bond (carbon adjacent to the pyridine ring), is shown in ref 3. For a vicinal coupling constant of 5.8 Hz, as is observed in the Zn^{2+} complex, a dihedral angle of 32.2° between H_C and H_E is predicted. If Φ_{CE} is 32.2°, then, assuming 120° between each substituent, Φ_{DE} is 87.8°. The Karplus equation predicts that $^3J_{DE}$ will be 0.27 Hz, which is too small to be observed. These dihedral angles are consistent with those determined by the X-ray crystal structures of [Zn-

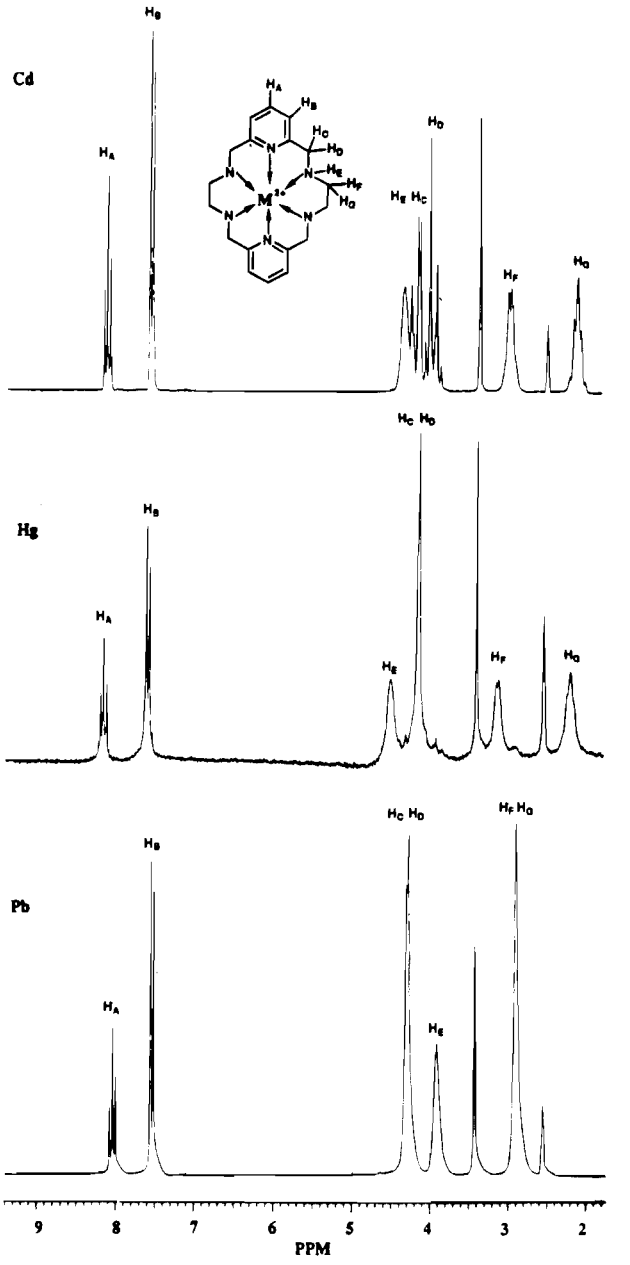

Figure 1. ^{1}H NMR spectra of Cd^{2+}, Hg^{2+}, and Pb^{2+} $(pyo)_2$[18]dieneN_6 complexes in DMSO-d_6 with internal TMS. DMSO and water impurity peaks are near 2.5 and 3.5 ppm, respectively.

(26) Cahn, R. S.; Ingold, C. K.; Prelog, V. *Angew. Chem., Int. Ed. Engl.* **1966**, *5*, 385−415.
(27) Pugmire, R. J.; Grant, D. M. *J. Am. Chem. Soc.* **1968**, *90*, 697−706.
(28) Ebsworth, E. A. V.; Rankin, D. W. H.; Cradock, S. *Structural Methods in Inorganic Chemistry*; Blackwell Scientific: Oxford, 1987; p 89.
(29) Emsley, J. W.; Feeney, J.; Sutcliffe, L. H., Eds. *High Resolution Nuclear Magnetic Spectroscopy*; Pergammon: London, 1966, Vol. 1, pp 357−363.
(30) Karplus, M. *Chem. Phys.* **1959**, *30*, 11−15.

$((pyo)_2[18]dieneN_6)]^{2+}$ and $[Cd((pyo)_2[18]dieneN_6)]^{2+}$, where Φ_{CE} is 31.8 and 28.4°, respectively, and Φ_{DE} is 84.8 and 89.5°, respectively. Approximately the same dihedral angles are indicated in the Mg^{2+} complex since no appreciable coupling between H_D and H_E is observed and the metal ion is approximately the same size as Zn^{2+}.

The hydrogens of the ethylenic linkages, H_F and H_G, are split into what appears at first inspection to be two complex multiplets. The COSY spectrum showed that each of these hydrogens is coupled to each other as well as to H_E. In a homonuclear proton decoupling experiment in which H_E is irradiated, the multiplets collapsed into an AA′BB′ spin system pattern. This is the same spin system observed[31-33] in $[Rh(en)_3]^{2+}$, $[Rh(en)_3]^{3+}$, $[Co(en)_3]^{3+}$, and the alkaline-earth complexes of a pyridine-containing macrocycle.[34] The same spin system was indicated by the spectrum of $[Zn((pyo)_2[18]dieneN_6)]^{2+}$, which could be simulated[35] by an AA′BB′XX′ spin system with the coupling constants obtained by application of the Karplus equation, using the dihedral angles derived from the crystal structure.

Comparing and contrasting the spectra of the Zn^{2+}, Cd^{2+}, and Mg^{2+} complexes in DMSO-d_6, the chemical shifts for hydrogens H_A and H_B are invariant to within 0.03 ppm, consistent with previous findings on coordinated pyridine.[36] The N−H resonance shifts upfield for the Cd^{2+} complex relative to the Zn^{2+} and Mg^{2+} complexes. When the temperature is raised from 298 to 363 K, the N−H resonance also shifts upfield reversibly for each complex. Since amine hydrogens which undergo hydrogen bonding shift downfield,[37] the observation of an upfield shift for the amine proton resonance in the spectra of the complexes upon raising the temperature implies a decrease in the extent of intermolecular hydrogen bonding with solvent as the temperature is increased.[38] For the Zn^{2+} and Mg^{2+} complexes, the hydrogens labeled H_C are more deshielded (4.33 and 4.32 ppm), relative to the same hydrogens in the Cd^{2+} complex (4.18 ppm). In contrast, the chemical shift of the other geminal hydrogen, H_D, is relatively invariant, appearing at 3.91 ppm for the Zn^{2+} and Mg^{2+} complexes and at 3.95 ppm for the Cd^{2+} complex. As expected, the geminal coupling constant between H_C and H_D is nearly the same for each complex.

It appears that as the macrocycle untwists to accommodate the larger Cd^{2+} ion, protons C, D, and E evolve from an ABX to an ABC spin system[29] at room temperature. But the invariance in the coupling constants indicates that the dihedral angles between the methylenic protons and the amine proton are approximately the same. Thus, the untwisting of the macrocycle to accommodate the larger Cd^{2+} ion must be accomplished, in part, by rotation about bonds other than the C−N bonds. It is also notable that this untwisting affects the chemical shifts more than the coupling constants.

It is well known that, in an ethylenediamine chelate ring in one conformation, δ or λ, there exists an effective chemical shift difference between each pair of geminal methylene protons, H_{axial} and $H_{equatorial}$, due to their disposition with respect to the N−M−N plane.[39] An *effective* chemical shift difference is observed since all $[M(en)_3]^{n+}$ and $[M(en)_2X_2]^{n+}$ complexes undergo rapid $\delta \rightleftharpoons \lambda$ conformational interconversions at room temperature. With small metal ions, one conformation is populated more of the time relative to the other conformation. Thus, the spectrum shows an AA′BB′ spin system for en complexes (in D_2O). As the M−N bond distance and the N−C−C−N dihedral angle increase for $[M(en)_3]^{n+}$ and $[M(en)_3X_2]^{n+}$ complexes, the en chelate ring becomes more puckered.[39] This increase in dihedral angle causes the axial protons to be more susceptible to the diamagnetic shielding arising from the metal ion, thus *increasing* the intrinsic chemical shift difference between H_{axial} and $H_{equatorial}$. Looking now at the chemical shift difference between the axial and equatorial protons of the $(pyo)_2[18]dieneN_6$ ethylenic linkages, H_G and H_F, for the Zn^{2+}, Mg^{2+}, and Cd^{2+} complexes, these are 0.65, 0.74, and 0.86 ppm, respectively, and thus are consistent with the increasing size of the metal ion. A change in the coupling constants is also expected as the metal size increases. However, calculations using the coupling constants and chemical shift differences for $[M(en)_3]^{n+}$ complexes indicated that coupling constant variations have a very small effect on the appearance of the spectrum.[39]

The hydrogens H_G have similar chemical shifts appearing at 2.10, 2.11, and 2.08 ppm for the Zn^{2+}, Cd^{2+}, and Mg^{2+} complexes, respectively. In contrast, the H_F hydrogens are shielded more in the Zn^{2+} complex, appearing at 2.75 ppm relative to the same hydrogens in the Mg^{2+} (2.82 ppm) and Cd^{2+} complexes (2.97 ppm). The axial hydrogens in the $[M(en)_3]^{n+}$ and $[M(en)_2X_2]^{n+}$ complexes appear at higher fields than the equatorial hydrogens.[31] Using the same orientations and dihedral angles observed in the crystal structure of $[Cd((pyo)_2[18]dieneN_6)]^{2+}$, the calculated spectrum obtained by spin simulation agrees with the experimental spectrum when the axial hydrogens, H_F, are assigned to a higher field than that of the equatorial hydrogens, H_G. When the crystal structures for the Zn^{2+} and Cd^{2+} complexes are compared, the N−C−C−N dihedral angle between the amine nitrogens (ω) increases from 63.5 to 69.8°, the angle between $C-H_{equatorial}$ and the $N_{amine}-M-N_{amine}$ plane remains constant at 10.7 and 10.9°, respectively, while the angle between $C-H_{axial}$ and the $N_{amine}-M-N_{amine}$ plane changes from 86.5 to 77.4°. These observations are consistent with assignment of the resonances with larger chemical shift differences to the axial protons and the resonances with invariant chemical shift to the equatorial protons. Thus, the ethylenediamine linkages of the macrocycle behave qualitatively analogous to en complexes when they adjust to increasing metal ion size.

The ^1H NMR spectral data for the Hg, Ca, Sr, and Pb complexes of $((pyo)_2[18]dieneN_6)$ in DMSO-d_6 are also given in Table 1. The chemical shifts for the pyridine hydrogens are similar to those for the pyridine hydrogens in the Zn^{2+}, Cd^{2+}, and Mg^{2+} complexes, differing by 0.1 to 0.2 ppm. In this group of larger metals, the spectrum of $[Hg((pyo)_2[18]dieneN_6)]^{2+}$ gives key information toward understanding the behavior of all the complexes, so it will be discussed in detail. The hydrogens labeled H_C, H_D, and H_E are coupled to one another, as confirmed by a COSY experiment, and constitute an ABC spin system. Unfortunately, the coupling constants between protons H_C and H_D could not be ascertained by a decoupling experiment where H_E is irradiated, since this resonance overlaps with the AB portion of the spin system. The coupling constants can be

(31) Beattie, J. K.; Elshernd, H. *J. Am. Chem. Soc.* **1970**, *92*, 1946−1948.
(32) Sudmeier, J. L.; Blackmer, G. L. *Inorg. Chem.* **1971**, *10*, 2010−2018.
(33) Sudmeier, J. L.; Blackmer, G. L.; Bradley, C. H.; Anet, F. A. *J. Am. Chem. Soc.* **1972**, *94*, 757−761.
(34) Dyer, R. B.; Palmer, R. A.; Ghirardelli, R. G.; Bradshaw, J. S.; Jones, B. A. *J. Am. Chem. Soc.* **1987**, *109*, 4780−4786.
(35) Bothner-By, A. A.; Castellano, S. J. *J. Chem. Phys.* **1969**, *41*, 3863−3869.
(36) Bombeieri, G.; Benetollo, F.; Polo, A.; DeCola, L.; Hawkins, W. T.; Vallarino, L. M. *Inorg. Chem.* **1991**, *30*, 1345−1353.
(37) Becker, E. D. *High Resolution NMR*; Academic: Orlando, FL, 1980; pp 256−258.
(38) Williams, D. H.; Fleming, I. *Spectroscopic Methods in Organic Chemistry*, 4th ed.; McGraw-Hill: London, 1987; p 137.
(39) Gollogy, J. R.; Hawkins, C. J.; Beattie, J. K. *Inorg. Chem.* **1971**, *10*, 317−323.

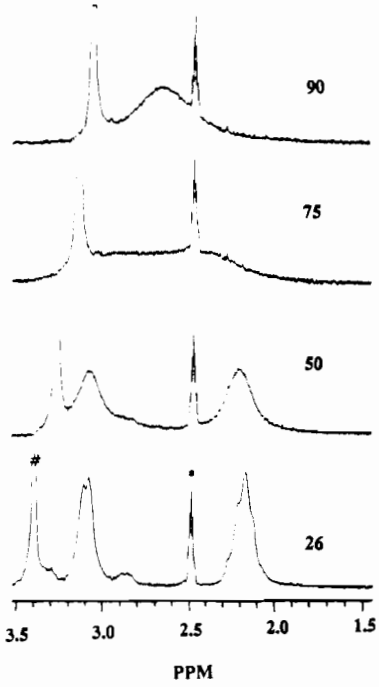

Figure 2. ^{1}H NMR spectra of ethylenic protons for $[Hg((pyo)_2[18]dieneN_6)]^{2+}$ in DMSO-d_6 at various temperatures (* denotes H_x-d_6-DMSO peaks and # denotes H_2O peak). The spectra are labeled with the temperature of the system.

obtained, however, from the complex dissolved in D_2O, where rapid NH/ND exchange occurs, resulting in an AB spin system (see below). The hydrogens H_F, H_G, and H_E are coupled to one another as confirmed by the COSY spectra. As is shown in Figure 2, increasing the temperature to 50 °C caused additional broadening of the proton resonances H_F and H_G. At 75 °C, these two resonances coalesced, and at 90 °C, they collapsed into a single resonance appearing at 2.65 ppm, the midpoint of the frequencies observed for the two separated resonances at 25 °C. This temperature dependence is due to the rate of δ to λ conformational interconversions of the ethylenic linkages relative to the time scale of the NMR experiment. When the temperature is 90 °C, the interconversion of the conformations of the ethylenic linkages is faster than the time scale of the NMR experiment. The result is a single resonance, similar to that observed for $[M(en)_3]^{n+}$ complexes.[39] The rate for the interconversion of the two conformations can be approximated by the equation[40] $\kappa_c = (\pi/\sqrt{2})\Delta\nu$, where $\Delta\nu = (\nu(H_F) - \nu(H_g))$ in Hertz at 26 ± 0.2 °C. Applying this equation to the data, a rate of 410 s^{-1} is obtained and the lifetime for the conformers is 2.43 ms. These calculations are only rough approximations since the equation involved gives reliable estimates only for coalescing doublets of AB spin systems.[41] No broadening is observed in the spectra of the smaller metal complexes (Zn^{2+}, Mg^{2+}, or Cd^{2+}) up to 90 °C. These results suggest that the rapid conformational interconversions in the Hg^{2+} complex are related to the larger size of Hg^{2+}, which causes the macrocycle to twist down less tightly and thus leads to a lower energy barrier for conformational interconversion.

The spectrum of $[Ca((pyo)_2[18]dieneN_6)](CF_3SO_3)_2$ in DMSO-d_6 shows a broad overlapping resonance for H_C/H_D centered at 3.86 ppm and a broad overlapping resonance for H_F/H_G centered at 2.75 ppm. The broad resonance for H_F/H_G appears at about the same chemical shift (2.65 ppm) as the analogous protons in the Hg^{2+} complex at 90 °C. Thus, it can be concluded that the interconversion of conformations for the ethylenic linkages is occurring rapidly at room temperature in the Ca^{2+} complex. The amine proton resonance, H_E, is shifted upfield by 1.32 ppm relative to the amine proton resonance in the Hg^{2+} complex. When the temperature is increased from 25 to 80 °C, the broad resonance for H_C/H_D sharpens and splits into a doublet (J = 4.8 Hz). Decoupling experiments at 80 °C, where the amine proton resonance H_E is irradiated, result in the collapse of the doublet into a singlet. This indicates that at higher temperature the protons H_C and H_D are undergoing fast interconversions but are still coupled to the vicinal amine hydrogen which is not undergoing rapid exchange. At 60 °C and above, the broad resonance for H_F and H_G sharpens into a singlet, indicating fast interconversion of ethylenic conformers. For the Sr^{2+} complex, the protons H_C and H_D have the same chemical shift and appear as a single sharp resonance at 25 °C. The proton resonances H_E, H_F, and H_G have the same chemical shifts and appear as a single sharp resonance at 2.75 ppm. For the Pb^{2+} complex, protons H_C and H_D have the same chemical shift but appear as a sharp doublet (J = 4.8 Hz). This resonance pattern is similar to that for the Ca^{2+} complex at 60 °C. Decoupling experiments on the Pb^{2+} complex where the amine proton, H_E, is irradiated caused the doublet to collapse to a singlet. The proton resonances H_F and H_G have the same chemical shift and appear as a single sharp resonance at 25 °C.

^{1}H NMR Spectra in D_2O. The ^{1}H NMR spectral data for Zn^{2+}, Cd^{2+}, Mg^{2+}, and Hg^{2+} complexes of $(pyo)_2[18]dieneN_6$ in D_2O are listed in Table 2. In contrast to the other complexes, the Mg^{2+} complex in D_2O with no free ligand added shows resonances attributable to both complexed and free macrocycle. The ratios of the intensities of these resonances do not vary significantly over a 2-week period; therefore, this complex is thermodynamically less stable than the others.

It was observed previously[3] that $[Zn((pyo)_2[18]dieneN_6)]^{2+}$ in D_2O has *no exchange* of N−H for N−D in D_2O over a 3-week period but that exchange could be induced by the addition of either DCl or NaOD. In contrast, the spectra of $[Cd((pyo)_2[18]dieneN_6)]^{2+}$ and $[Mg((pyo)_2[18]dieneN_6)]^{2+}$ in D_2O indicate that these two complexes do undergo rapid NH/ND exchange in neutral solution. The rapid NH/ND exchange is a reflection of the decreased stability of the Mg^{2+} complex compared to that of the Zn^{2+} complex and, in the case of Cd^{2+}, the increased kinetic lability of the N-H bonds when the macrocycle binds to the larger Cd^{2+} ion.

The spectrum of the Hg^{2+} complex dissolved in D_2O indicates that NH/ND exchange has occurred, which results in the H_C and H_D protons forming an AB spin system (see Table 2). This exchange allows the determination of the coupling constant between H_C and H_D (J = 16.8 Hz), which is similar to that obtained for the Zn^{2+}, Cd^{2+}, and Mg^{2+} complexes (J = 17.0 Hz), as is expected for geminal hydrogens. The hydrogens labeled H_F and H_G constitute an AA′BB′ spin system, which was verified by spin simulation of the experimental spectrum. The coupling constants for protons H_F and H_G in the spectrum of the Hg^{2+} (J = 10.6 Hz) are similar to those for the Cd^{2+} and Mg^{2+} complexes (10.6 and 10.4 ppm, respectively).

The chemical shift differences between protons H_C and H_D and protons H_F and H_G for the Hg^{2+}, Zn^{2+}, Mg^{2+}, and Cd^{2+} complexes are given in Table 3. As the metal ion increases in size going from Zn^{2+} to Hg^{2+}, the chemical shift difference between protons H_C and H_D *decreases*. This decrease causes the resonances of the AB quartet to come closer together, resulting in a decrease in intensity for the two outer lines relative to the two inner lines. In contrast, as the size of the metal ion

(40) Gutowsky, H. S.; Holm, C. H. *J. Chem. Phys.* **1956**, *25*, 1228−1234.
(41) Kost, D.; Carlson, E. H.; Raban, M. *J. Chem. Soc., Chem. Commun.* **1971**, 656−657.

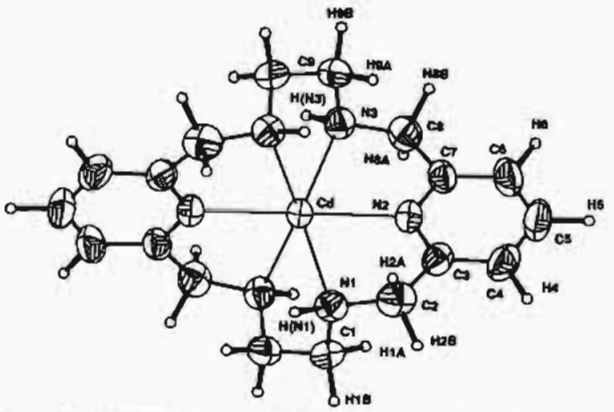

Figure 3. ORTEP diagram of $[Cd((pyo)_2[18]dieneN_6)]^{2+}$.

increases, the chemical shift difference between protons H_F and H_G *increases*. Thus, untwisting of the macrocycle to accommodate the larger metal ions results in an increase in the N−C−C−N dihedral angle and an increase in the chemical shift difference between geminal hydrogens of the ethylenic linkages.

X-ray Crystal Structure of $[Cd((pyo)_2[18]dieneN_6)](CF_3SO_3)_2$. In order to better understand the structural features of $(pyo)_2[18]dieneN_6$ when coordinated to metal ions of different sizes, a crystallographic analysis of $[Cd((pyo)_2[18]dieneN_6)](CF_3SO_3)_2$ was performed. Zn^{2+} and Cd^{2+} differ in size by 0.21 Å (six-coordinate ionic radii). Recrystallization of $[Cd((pyo)_2[18]dieneN_6)](CF_3SO_3)_2$ from water gave colorless monoclinic crystals containing no solvent. The crystallographic summary is given in Table 4. The ORTEP diagram of $[Cd((pyo)_2[18]dieneN_6)]^{2+}$ is shown in Figure 3. In the crystal lattice, the cadmium atom sits at a site of 2-fold symmetry. The relative positions of the hydrogen atoms on the amines correspond to ligand isomer V (ref 3) and the macrocycle is twisted in a helical shape, with the two pyridine rings oriented at 91.5° relative to each other (compared to 104.5° for Zn^{2+}). The twisting of the macrocycle gives rise to two meridional linkages, each incorporating a pyridine nitrogen and the two adjacent aliphatic amines. The coordination sphere is distorted in that two *trans* aliphatic amines of one meridional span are displaced 0.754 Å above the equatorial plane while the other two *trans* aliphatic amines are an equal distance below the plane (compared to 0.567 Å in the Zn^{2+} complex). A similar distortion was observed for various $[M[18]aneN_2S_4]^{x+}$ complexes.[42] The helical shape of the molecule is easily visualized by examining a space-filling model drawn with the crystallographic coordinates as shown in Figure 4.

Selected bond distances and angles are listed in Table 6. The two $Cd-N_{py}$ distances are 2.306(4) Å, and the four $Cd-N_{am}$ distances are pairwise equivalent by symmetry at 2.382(5) Å (N1, N1a) and 2.372(4) Å (N3, N3a). These distances are larger by 0.19 and 0.17 Å when compared to the analogous distances in the Zn^{2+} complex, as is expected from the relative ionic radii. The longer $Cd^{2+}-N_{am}$ bond distances when compared to the $Cd^{2+}-N_{py}$ bond distances are also as expected.[43] The $Cd^{2+}-N_{am}$ bond distances are slightly shorter than those observed in the Cd^{2+} complex of a quinquedentate macrocycle derived from the condensation of diacetylpyridine and triethylenetetraamine (2.43 Å).[44] Comparison of the $Cd^{2+}-N_{am}$ band distance of the $Cd^{2+}-N_{py}$ bond distance in the same complex also shows that this distance is also shorter by approximately 0.03 Å than in the quinquedentate macrocyclic complex. However, the $Cd^{2+}-N_{am}$ distances are almost the same as those observed in $[Cd(en)_3]^{2+}$ (2.361, 2.371, 2.347, 2.377, 2.385, and 2.392 Å).[45] The triflate counterions refined with no disorder, giving bond distances and angles typical for that ion.

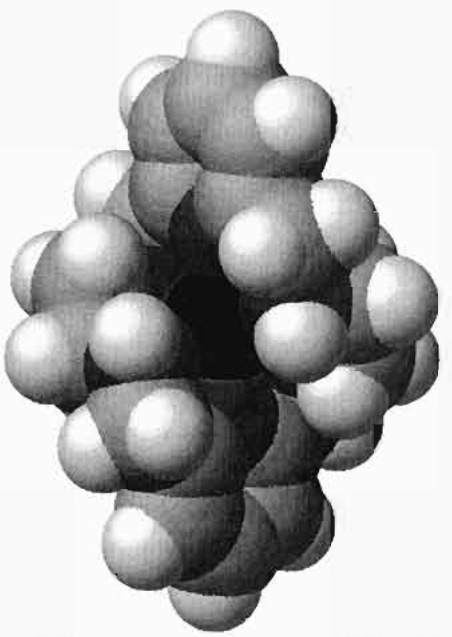

Figure 4. Space-filling model representation of the crystal structure of $[Cd((pyo)_2[18]dieneN_6)]^{2+}$.

The twist of $(pyo)_2[18]dieneN_6$ about Cd^{2+} gives rise to $\Lambda\delta\delta$ and $\Delta\lambda\lambda$ isomers. The C−C bond distances of 1.505(8) Å for the ethylenic chelate rings within the macrocycle are in the reported range of 1.41 to 1.57 Å for ethylenediamine complexes[46] and close to the distance, 1.509 Å, observed for the Zn^{2+} complex. The conformation of the diaminoethane chelate rings within the macrocycle is gauche[47,48] as defined by an $N_{am}-C-C-N_{am}$ dihedral angle of approximately 50°. This dihedral angle is 63.5° in $[Zn((pyo)_2[18]dieneN_6)]^{2+}$ and 69.8° in $[Cd((pyo)_2[18]dieneN_6)]^{2+}$. A second criterion defining the gauche conformation is that the angle between the plane defined by the metal ion and the two nitrogen atoms and the plane defined by the metal ion and the two carbon atoms should be greater than 0°. This angle is 32 and 33° in the Cd and Zn complexes, respectively. The final criterion, that the two carbon atoms are symmetric above and below the $M-N_{am}-N_{am}$ plane, is also observed in both cases.

For $M(en)_2$ complexes, there are six possible conformational isomers, $\Lambda\lambda\lambda$, $\Lambda\delta\delta$, $\Lambda\delta\lambda$, $\Delta\lambda\lambda$, $\Delta\delta\delta$, and $\Delta\delta\lambda$.[48] But, from the symmetry of $[Cd((pyo)_2[18]dieneN_6)]^{2+}$, only the isomers $\Lambda\lambda\lambda$, $\Lambda\delta\delta$, $\Delta\lambda\lambda$, and $\Delta\delta\delta$ are possible. Since the space group $I2/m$ is centrosymmetric, the crystals consist of a racemic mixture corresponding to one of the two pairs of enantiomorphs, either ($\Lambda\lambda\lambda$, $\Delta\delta\delta$) or ($\Lambda\delta\delta$, $\Delta\lambda\lambda$). Examination of Figure 3 shows that the latter pair of enantiomorphs is present in the crystal. The presence of a racemic mixture was confirmed in the case of Zn^{2+} by the experimental optical resolution of the enantiomers. No attempt has been made to resolve the isomers of $[Cd((pyo)_2[18]dieneN_6)]^{2+}$.

(42) Reid, G.; Schröder, M. *Chem. Soc. Rev.* **1990**, *19*, 239−269.
(43) Melson, G. A., Ed. *Coordination Chemistry of Macrocyclic Compounds*; Plenum: New York, 1979; p 268.
(44) Drew, M. G. B.; McFall, S. G.; Nelson, S. M. *J. Chem. Soc., Dalton Trans.* **1979**, 575−581.
(45) Breitwieser, M.; Gottlicher, S.; Paulus, H. *Z. Kristallogr.* **1984**, *166*, 207−212.
(46) Muralikrishna, C.; Mahadevan, C.; Sastry, S.; Seshasayee, M.; Subramanian, S. *Acta Crystallogr., Sect C.* **1983**, *39*, 1630.
(47) Raymond, K. N.; Cornfield, P. W. R.; Ibers, J. A. *Inorg. Chem.* **1968**, *7*, 842−844.
(48) Cullen, D. L.; Lingafelter, E. C. *Inorg. Chem.* **1970**, *9*, 1858−1864.

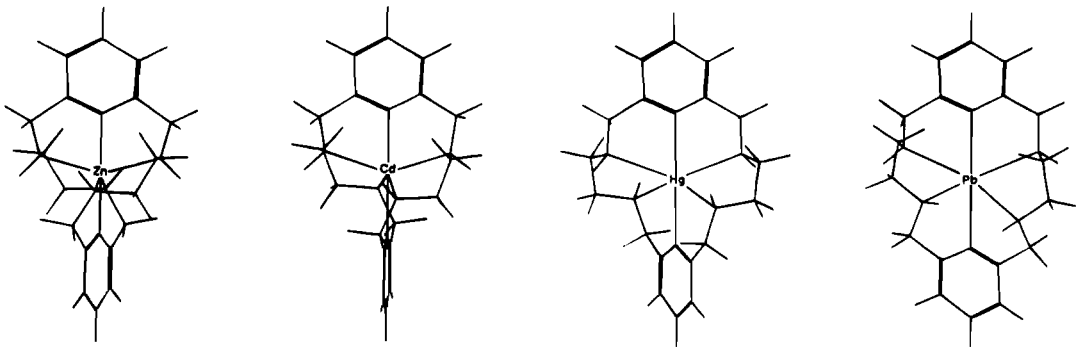

Figure 5. Comparison of structures of Zn^{2+}, Cd^{2+}, Hg^{2+}, and Pb^{2+} $(pyo)_2$[18]dieneN_6 complexes as calculated by MMX in PCMODEL.

Molecular Modeling. The structures of the Zn^{2+} and Cd^{2+} complexes of $(pyo)_2$[18]dieneN_6 are modeled very well by MMX in PCMODEL with the parameter set and interactions described above in the Experimental Section (see Figure 5). The calculated angles are within 1° of the crystallographic angles, and the distances are within 0.02 Å in most cases. The calculated models of the Hg^{2+} and the Pb^{2+} complexes have no structural comparison, but it will be seen that they continue the trends of the Zn and Cd complexes, giving results consistent with the observed NMR spectra.

The methylenic substituent carbons of pyridine in $(pyo)_2$[18]-dieneN_6 form the termini of two chains of atoms, including the ethylenediamine moieties, that form a double helix about Cd, connecting the 2- and 6-positions of the *trans* pyridine groups (see Figure 4). The helical conformation is achieved through rotation about single bonds, chiefly the C1−C9a bond of the en group and the $C_{py}-C_{methylenic}$ (C3−C2) bonds. Furthermore, the helical linkages must be held rigidly by coordination since the ^1H NMR patterns give exquisite evidence for the absence of fluctional motion or averaging of coupling constants. The untwisting of the macrocycle to accommodate the larger Cd^{2+} ion relative to Zn^{2+} is achieved by rotation about C1−C9a to increase the $N_{am}-N_{am}$ bite distance from 2.91 Å for Zn to 3.00 Å for Cd and the $N_{am}-C-C-N_{am}$ dihedral from 63.5 to 69.8°. These changes are consistent with the observation that the chemical shifts of H_F and H_G (H1a and H1b) become farther apart as metal ion size increases (see NMR section above). This rotation also forces the meridional spans farther apart and decreases the helicity of the macrocyclic topology. A measure of the helicity of an ideal helix is the angle between the axis of the helix and a tangent to the helix. This angle is approximated in $(pyo)_2$[18]dieneN_6 by the angle between the $N_{py}-M-N_{py}$ axis (axis of the "helix") and the plane formed by the M and two carbon atoms of the ethylenic linkage. This angle decreases from 45 to 36° in the Zn and Cd structures, respectively, and is predicted to further decrease to 26 and 8° in the calculated Hg and Pb structures. Similarly, the angle between the planes of the two pyridine groups also decreases as the helix untwists, from 105 to 91° for Zn and Cd and to 77 and 30° predicted for Hg and Pb.

The bite distances of the $N_{am}-C-C_{py}-N_{py}$ chelate rings also increase, from 2.63 Å for Zn to 2.73 and 2.74 Å for Cd. Interestingly, this increase is accomplished by rotation about C3−C2 to *decrease* the $N_{am}-C-C_{py}-N_{py}$ dihedral angle from 26.9° for Zn to 25.3 and 25.0° for Cd. This ultimately causes the $N_{am}-C-C_{py}-N_{py}$ chelate ring to become eclipsed in the limit of large metal ions with the consequence that H_C and H_D (H2a and H2b) are symmetric with respect to the plane of the pyridine ring and therefore approach each other in chemical shift. This effect is consistent with the observation that protons C and D have decreasing chemical shift difference and are equivalent for metal ions the size of Ca or larger. This effect is also predicted in the molecular mechanics calculated structures of the Hg and Pb complexes shown in Figure 5. In this figure, the four calculated structures are presented for comparison with the top pyridine group in the plane of the paper. By comparing the bottom pyridine groups it can be seen that in the case of Zn the twist is past 90°, it is equal to 90° for Cd, and it is less than 90° for Hg and Pb. Rotations about all of the $C-N_{am}$ bonds are also necessary when the metal ion size is increased in order to keep the amine nitrogen lone pairs pointing at the center of the macrocyclic cavity. However, these rotations are small enough that they do not cause observable differences in the coupling constants between the N−H and C−H groups. As a result, the chemical shifts of the methylenic protons are the most sensitive indicator of changes in the macrocyclic conformation as the size of the metal ion increases.

Acknowledgment. The authors thank Dr. Peter White at UNC-Chapel Hill for assistance with the crystal structure. S.C.J. thanks her hosts at Battelle Pacific Northwest Laboratories, Dr. Dennis Wester and Dr. Benjamin Hay, for helpful discussions on molecular modeling. This research was partially supported by grants from the National Science Foundation (CHE-9308988) and the National Institutes of Health (GM-41919).

Supporting Information Available: Listings of anisotropic thermal parameters, bond distances, bond angles, and torsion angles (9 pages). Ordering information is given on any current masthead page.

IC9413427